J Petrol Explor Prod Technol (2017) 7:417–432
DOI 10.1007/s13202-016-0301-3

ORIGINAL PAPER - EXPLORATION GEOPHYSICS

2D and 3D seismic simulation for fault modeling: exploratory revision from the Gullfaks field

Numair A. Siddiqui[1] · Manoj. J. Mathew[2] · David Menier[2] · M. Hassaan[1]

Received: 13 October 2014 / Accepted: 2 November 2016 / Published online: 21 November 2016

Abstract 2D and 3D seismic data have emerged as a key tool in the oil and gas industry to visualize and understand subsurface morphology and boundaries. In addition to providing excellent structural images, the dense sampling of 2D and 3D survey can sometimes make it possible to map reservoir quality and the distribution of hydrocarbon with well-marked limitations. Here we use 2D and 3D seismic data to map and interpret basic structures and fault lines to construct 2D and 3D base fault models of the Gullfaks field, while avoiding common pitfalls. This work also highlights important concepts and principles that allow selection, interpretation and simulation of particular areas containing hydrocarbon traps through the comparison of different maps such as time structure, amplitude and coherence. The field covers an area of approximately 50 km^2 entirely confined within block 34/10 in the Norwegian sector of the North Sea. The area of the seismic lines extends to 4875 m laterally and vertically up to 4.5 s. Based on all the selected horizons, constructed maps and dominant fault construction models (2D and 3D), we show the presence of a major fault that cuts five horizons of the area of interest. The structural features include antiform and a set of extensional faults with master, antithetic and synthetic faults with opposite sense of shear (dip direction and angle $\sim 60°$). Ductile deformation at the bottom of seismic lines shows the fluctuation of amplitude of acoustic signals in seismic lines. Our results demonstrate uplift along the major fault during extension indicated by chaotic distortion at the bottom, which reveals a gas trap. In the Gullfaks field, termination of fault movement and subsequent deformation appears to have occurred for a long period of time. This illustrates the use of 2D and 3D visualization with horizon attributes that can conveniently provide massive amounts of data which elucidates the trapping mechanism of faults.

Keywords Seismic attributes · Fault interpretation · Horizon attributes maps · 2D/3D modeling · Gullfaks field

Introduction

Understanding subsurface geology is of paramount importance to discover hydrocarbon-bearing reservoirs and efficiently extract the hydrocarbon. At its simplest, this means mapping and interpreting subsurface architecture to identify structures within which oil and gas may be trapped, or mapping faults that may serve as barriers or conduits to oil flow in a producing field (Anderson 1951; Sebring 1958; Perkins 1961). Quality analysis of subsurface interpretations can be facilitated and enhanced by construction of detailed maps such as time-thickness maps, dip maps, amplitude maps among others. These assist to estimate the volume of hydrocarbon that may be present in a given trap, and partly to plan the best possible technique to extract the oil or gas. It could be utilized to detect accumulations of oil and gas in the subsurface, and this would reduce the risk of drilling an unsuccessful exploration well (Smalley et al. 2008). An essential tool implemented in oil and gas industries includes 2D and 3D seismic models, which can be used to improve our

✉ Numair A. Siddiqui
numair.siddiqui@utp.edu.my

[1] Department of Geoscience, Faculty of Geoscience and Petroleum Engineering, Universiti Teknologi PETRONAS, Tronoh, Perak, Malaysia

[2] GMGL UMR CNRS 6538, Université de Bretagne Sud, 56017 Vannes Cedex, France

understanding of subsurface structures for the economic recovery of oil and gas (Bacon et al. 2007).

The Gullfaks field covers an area of approximately 50 km^2 entirely confined within block 34/10 in the Norwegian sector of the North Sea (Petterson et al. 1992; Yielding et al. 1999; Norwegian Petroleum Directorate 2007) which is located on the Western margin of the Viking Graben of the North Sea rift system. The Gullfaks is one of the four important areas of the North Sea, due to the fact that it has dominated Norwegian oil production up to the mid-1990s (Bækken and Zenker 2007). Gullfaks was discovered in 1978 following the award of the concession to the group comprising Statoil (operator), Norsk Hydro and Saga Petroleum (Statoil Hydro 2007). Production commenced in December 1986 and is expected to continue for more than 30 years (Erichsen et al. 1987).

The oil entrapments are believed to be fault seal related (Milnes and Storli 1992). Because of its position, this area geologically (especially structural geology) has attracted much interest over the last decade (Fossen 1989; Petterson et al. 1990; Koestler et al. 1994; Fossen and Rornes 1995; Fossen and Hesthammer 1998, 2000). The area also contains the highest density of geological data in the North Sea rift system (Beach 1986), including a large amount of 3D seismic survey, deep sea profiles and dipmeter data, in addition to cores and other information from about more than 150 exploration and production wells (Petterson et al. 1990; Zanella and Coward 2003). The large and still growing amount of data makes the area well suited for detailed structural analysis to understand upper crustal extensional deformation in rift system.

In this work, part of 3D cube data with 2D maps were used to understand the deformation and evaluation of the structural traps, and as a result, fault models were developed consecutively in Gullfaks field within block 34/10 in the Norwegian sector of the North Sea to demonstrate fault modeling. The area of the seismic lines extended to 4875 m laterally and vertically up to 4.5 s.

Gullfaks oil field

Gullfaks is a giant oil field in the north of the Norwegian North Sea in block 34/10, approximately 175 km northwest of Bergen with an aerial extent of 50 km^2 (Norwegian Petroleum Directorate 2007) (Fig. 1).

The field came on stream in 1986, and the production up to June 2007 amounted to 2.09 × 109 bbl. (from: Norway Ministry of Petroleum and Energy). The sandstone reservoir units are of Early and Middle Jurassic age located at depth of 2000 m subsea and several hundred meters thick. The field is of good reservoir quality and generally possesses high permeability which represents 93% of the base reserves, assuming today's expected recovery factor of 61% (Anthony et al. 2008).

The ultimate goal is to achieve a recovery factor of 70%, and 3D seismic interpretation is a key element in locating the remaining oil to achieve this. However, presently this

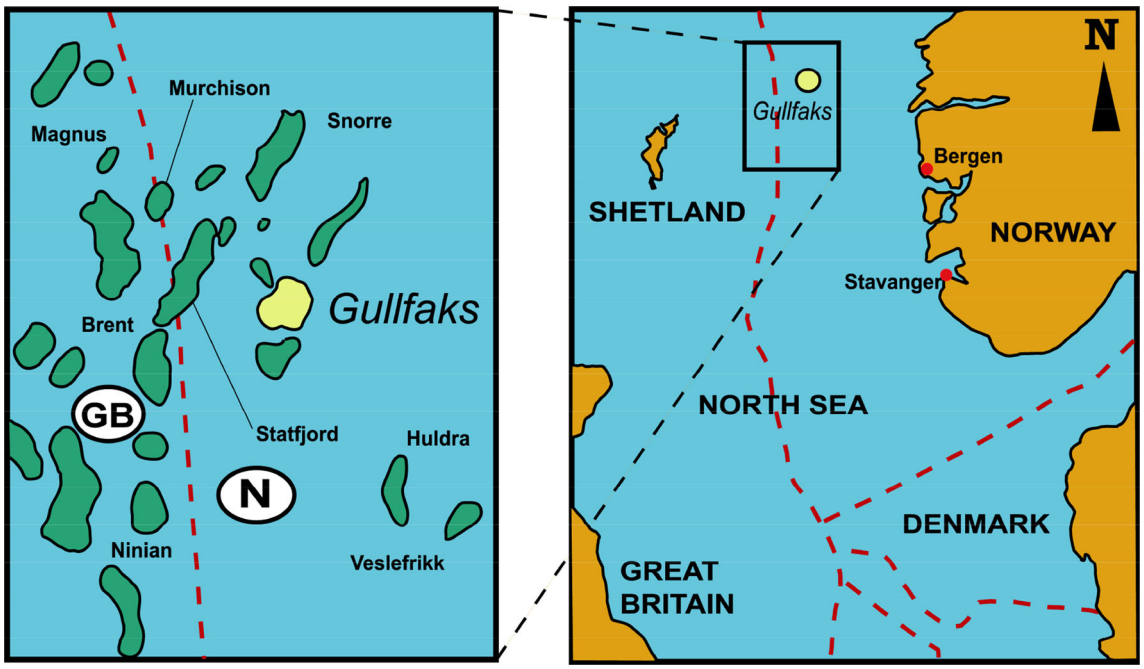

Fig. 1 Location of Gullfaks field, North Sea (after: Arild and Petter 2000)

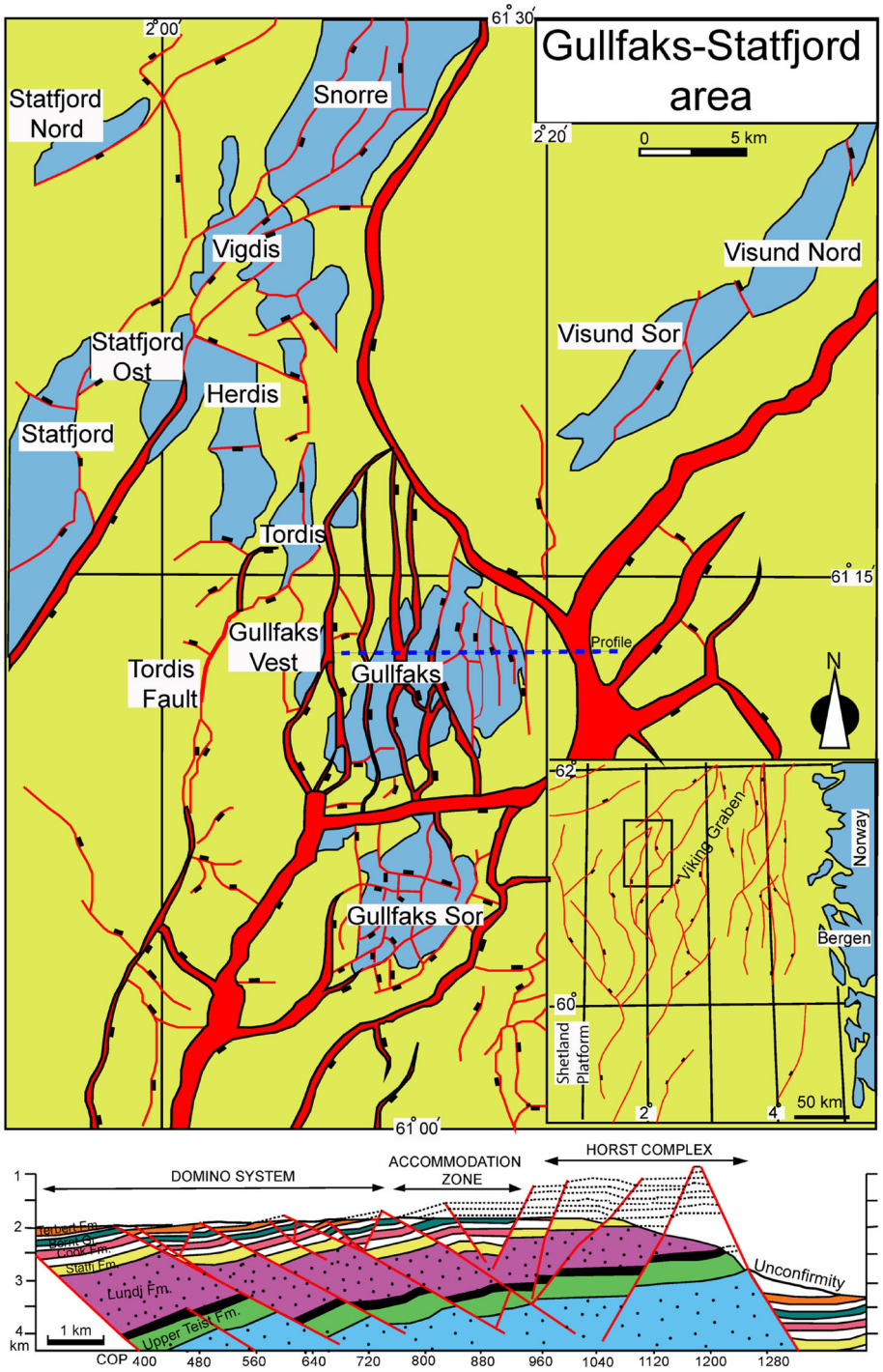

Fig. 2 Structural map and cross section of the Gullfaks field (from: Yielding et al. 1999)

overpressure field is on the decline and produced mostly through water injection and to a lesser degree by natural water.

Regional geology and tectonism

The Gullfaks field resides within the Viking Graben on its western flank in a complex series of dipping fault blocks (Fig. 2). Fossen and Hesthammer (1998) mentioned that its extensional history dated back to the Devonian phase succeeding the Caledonian collision. It was also mentioned that the rifting phases consisted of two, the Permo-Triassic and the Late Jurassic phases, with the latter being more apparent in seismic data. The base of the Gullfaks field is the Cretaceous unconformity (with a time gap of 100 Ma) which separates the Upper Cretaceous sediments from the

Jurassic or Triassic sediments (Evans et al. 2003). Wensaas et al. (1994) mentioned that early Cretaceous sedimentation was influenced by the Late Kimmerian tectonic phase suffering erosion of structural highs. He also added that most of the Upper Jurassic and Lower Cretaceous sediments are largely absent from the main Gullfaks structure, hence reinforcing the point made by Fossen and Hesthammer (1998), earlier and also since the Upper Cretaceous times, the whole area has been subsiding.

Structurally, the field is very complex and can be divided into three regions; the 'Domino System' bounded by low dipping rotated fault blocks in the west, a horst in the east, both sandwiching an 'Adaptation zone' characterized by fold structures (Fossen and Hesthammer 1998). The Domino System contains fault blocks trending N–S and dips of 30 degrees which are compartmentalized by smaller faults with variable trends (Fossen and Hesthammer 1998). The horst on the eastern side slopes downward to the west (Fig. 2).

The field is trapped in a series of rotated fault blocks defined by major N–S trending faults, with throws up to several hundreds of meters (Rouby et al. 1996) (Fig. 2). The secondary fault system trends in E–W with smaller throws of up to 100 m. The reservoirs consist of Cretaceous, Jurassic and Triassic sandstones.

Subsidence occurred throughout the Triassic, when 3000 m of Triassic sediments was deposited in the northern Viking Graben (Gabrielsen et al. 1990). A major uplift is recorded in the Lower–Middle Jurassic series of the central North Sea, where a major rift dome was located. In the northern Viking Graben, doming-related regression led to the deposition of the Middle to the Late Jurassic (Arild and Petter 2000).

The Shetland Platform was uplifted, and differential fault block subsidence was associated with the development and rotation of large fault block, with the Late Jurassic rifting phase constituting the major contributor to the structuring of Jurassic–Triassic reservoir which are very pronounced on seismic data and of greatest importance for the oil industry (Rouby et al. 1996; Anthony et al. 2008).

The rate of extension decreased in the Early Cretaceous. Thermal subsidence appears to have influenced the entire North Sea until the Paleocene. A general rise in sea level resulted in progressive overstepping of the platform and burial of the Jurassic fault block during the Cretaceous (Rouby et al. 1996).

Methodology

Interpretations were made on a 3D seismic cube providing full-volume visualization. In order to perform interpretations, initial steps of constructing horizons at varying depths and fault identification are carried out using the Kingdom Suite software 8.8. Generation of time structure/amplitude/coherence and time-thickness maps was constructed from the determined horizons. Depositional features of different bed forms were identified from the seismic attributes. Fault identification is a crucial step that was carried out simultaneously in order to categorize the faults and create fault surfaces. Integrating these data would aid in identifying hydrocarbon traps in the region, and by utilizing these data sets, 2D and 3D models were constructed (Fig. 3).

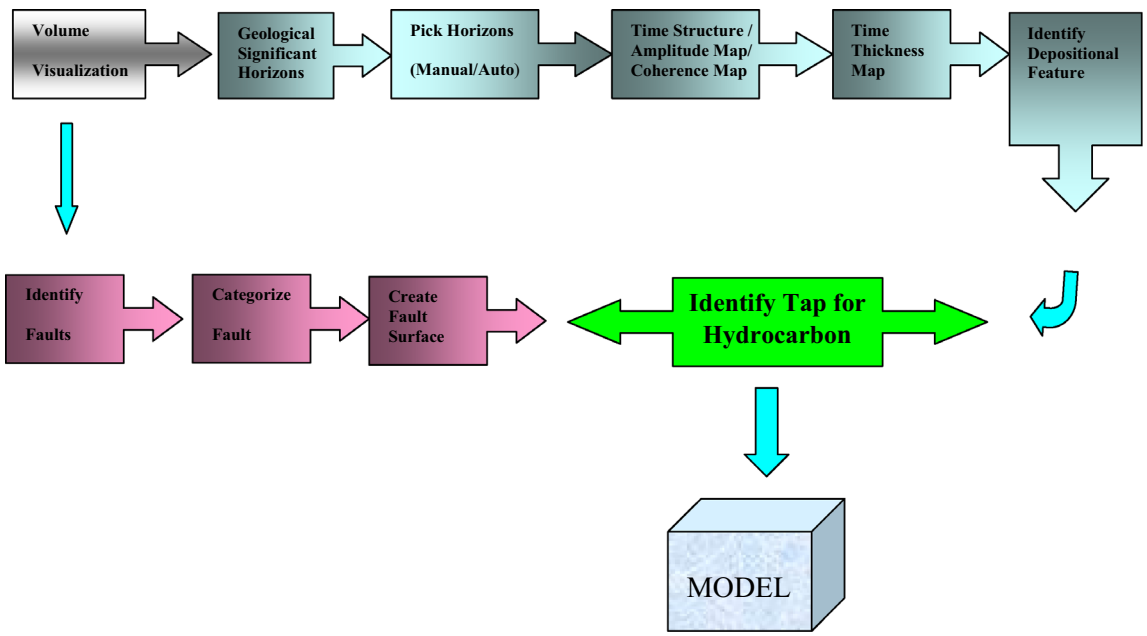

Fig. 3 Workflow diagram for 2D and 3D fault modeling

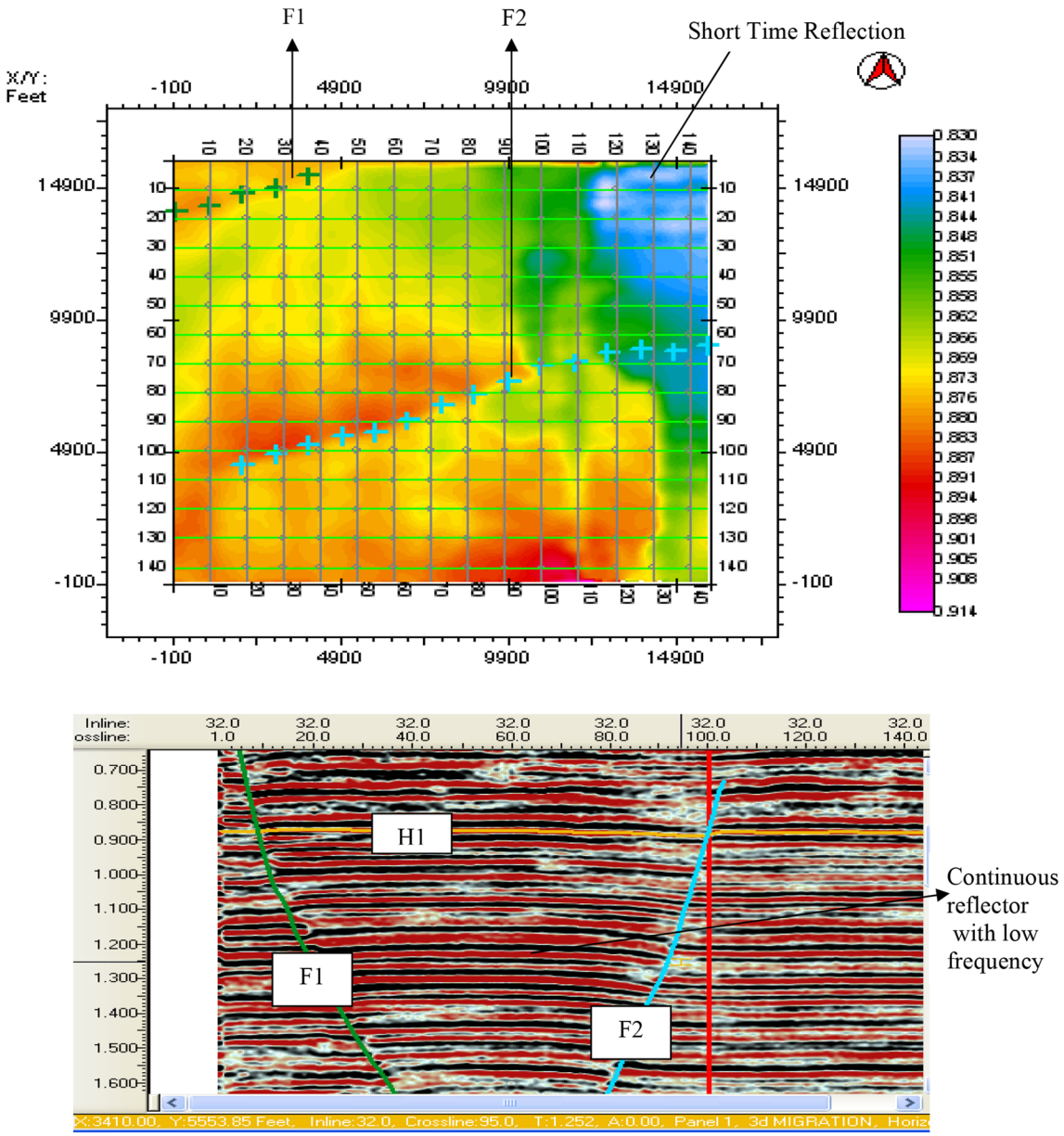

Fig. 4 Travel time of horizon H1 at 0.90 s., with faults F1 (*green*) and F2 (*blue*), mostly continuous reflection with high amplitude and low frequency

Flowchart

See Fig. 3.

Results and discussion

The 3D seismic data are divided into five horizons (H1–H5) and five faults (F1–F5). The upper part of the seismic block shows very low amplitude owing to the process of seismic wave generation. Middle section, i.e., at time from 0.4 to 3 s, is mostly high amplitude and continuous. In the deeper part, the reflections are mostly moderately chaotic and strenuous to correlate due to complexity of geology and faults with low amplitude, which are the results of sediment over sand having gas trapped at 1800 ft (−0.28) or could be muddy sand. In input 3D cube data, following results have been determined with the help of time structure maps, coherent maps, time-thickness maps, amplitude maps, amplitude window map and contour maps;

- Faults (dip and strike, master fault, antithetic fault and synthetic fault).

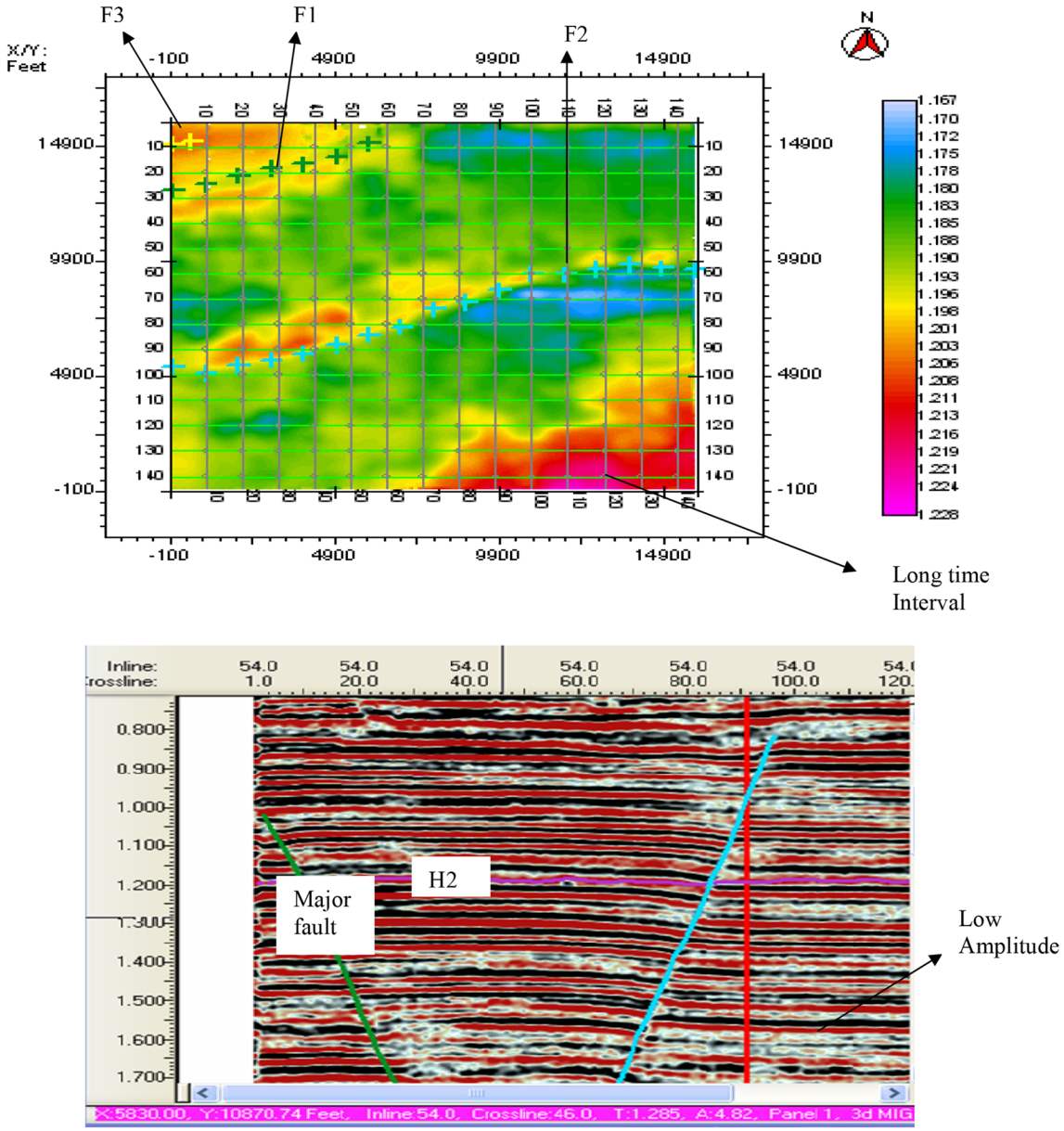

Fig. 5 Travel time of horizon H2 at 1.2 s., with faults F1 (*green*), F2 (*blue*) and F3 (*yellow*), mostly continuous reflection (discontinuous with fault) with high and low amplitudes

- Dip angle of fault is about 60°.
- High amplitude mostly to low.
- Moderate chaotic profiles.
- Continuous reflector to poorly.
- Uplifts and wavy beds.
- Stratigraphic traps.

Time structure maps

The main features of this time structure map are constant and continuous reflection in the top three horizons (Figs. 4, 5, 6) and some uplift within the E to SE corner at the bottom of the reflection. Small antiform shape is not clearly defined, and the uplift is considered to be related to the local topographic high due to fault and possible gas migration from deeper geology forming a chimney type of structure with chaotic reflection observed below the antiform structure (Figs. 7, 8).

In comparison with fault, the F1 cuts across five horizons and is referred as the master fault. Fault F2 is antithetic that cuts horizon H1, H2 and H3, whereas fault F3 is synthetic that cuts horizon H2, H3 and H4.

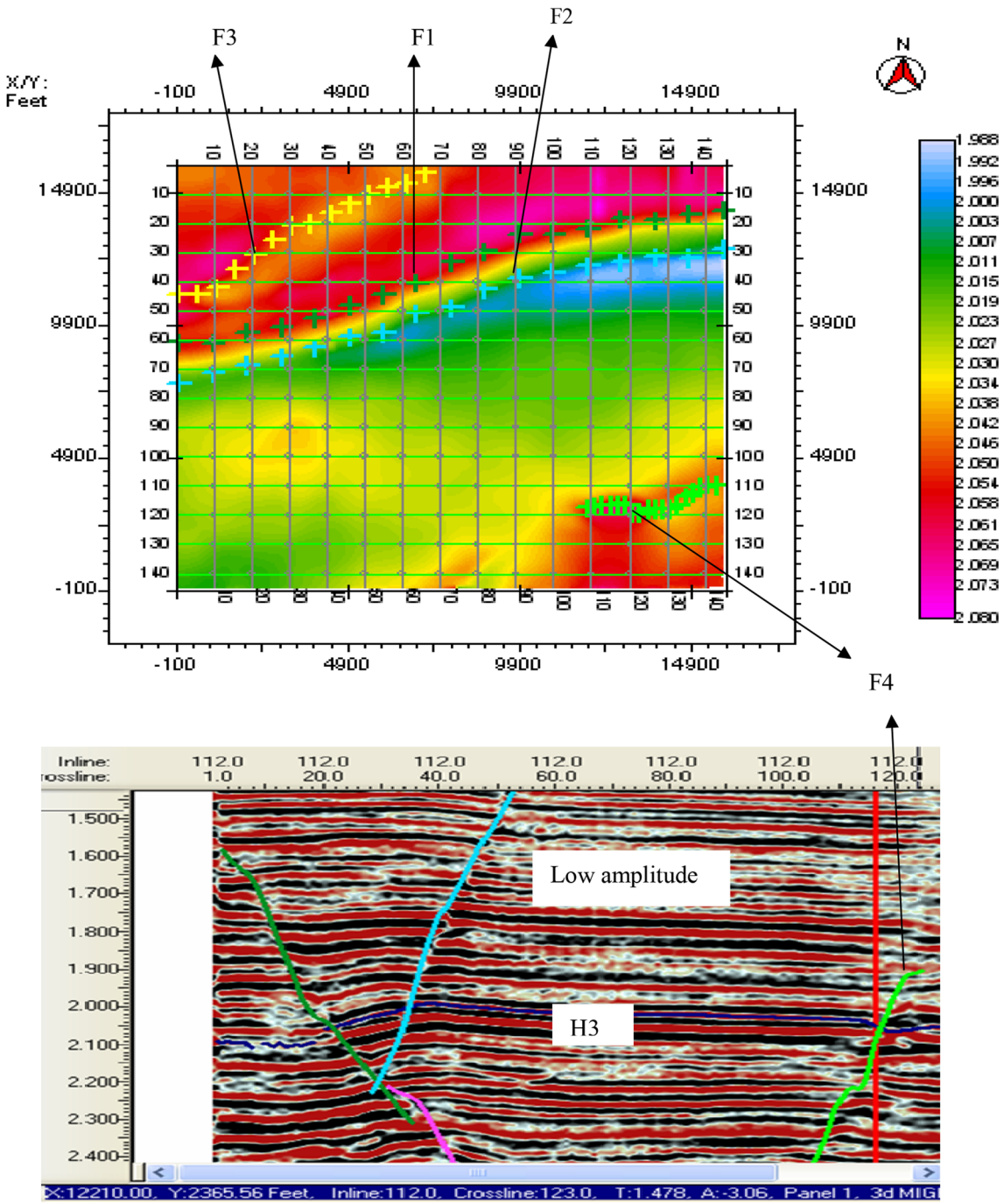

Fig. 6 Travel time of horizon H3 at 2.1 s., with faults F1 (*green*), F2 (*blue*), F3 (*yellow*) and F4 (*light green*), mostly continuous reflection (discontinuous with fault) with high and low amplitudes

The characteristics of the map are:

- It shows the time at which the seismic waves reflected through any horizons (TWT).
- Colors indicate travel times.
- Artificial lighting shows shadows.
- At depth, the time structure may vary from the true geological structure.
- Useful preliminary visualization of the subsurface.

Amplitude maps

A new approach to seismic interpretation improves resolution and reduces risk.

Spectral decomposition is a simple yet robust approach for generating high-resolution seismic images of stratigraphic and structural prospects of reservoirs. The images are based on amplitude response, the most powerful

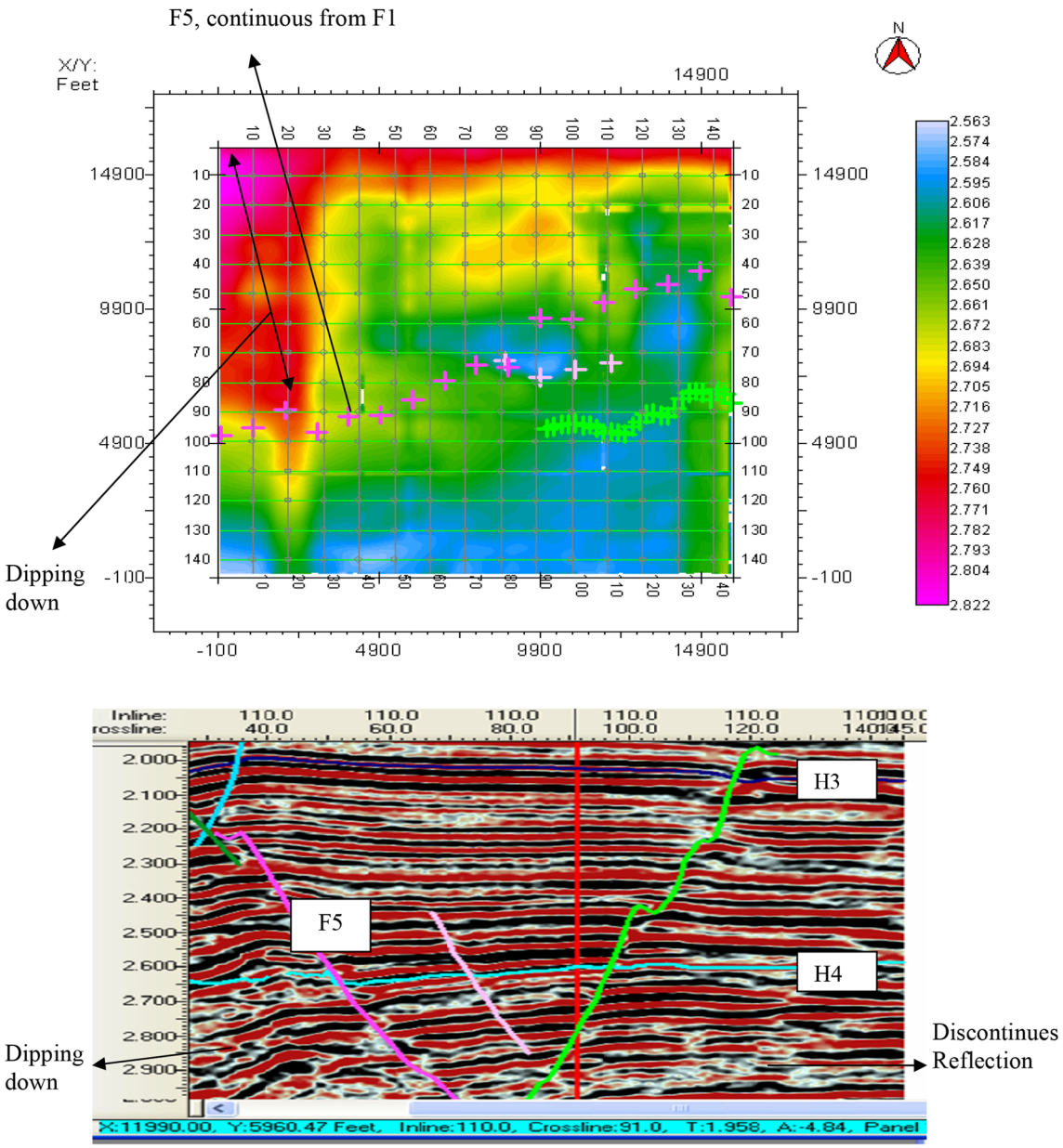

Fig. 7 Travel time of horizon H4 at 2.65 s., with all faults, continuous to discontinuous reflection with high and low amplitudes. F5 and F4 cutting the horizon

seismic attribute, yet these unique images provide far greater resolution of reservoir boundaries, reservoir heterogeneities and thickness than is possible with traditional broadband seismic displays. Characteristics of spectral decomposition images typically relate more directly to reservoir heterogeneity than complex trace attributes.

The amplitude map shows the following characteristics.

- Amplitudes vary with geology.
- Can show different sediment bodies.
- Amplitude anomalies (low or high) can result from: A sand body often gives a high-amplitude response on grain size, porosity, fluid content, geometry, source frequency, sediment heterogeneity plus other factors.
- High amplitudes can result from muddy sand, sandy mud, porous mud/sand, basalt, salt, coal.
- Low amplitudes can result from well-sorted sand.

Amplitude map between H3 and H2

The typical amplitude map from all five horizons is in between H3 and H2 (Fig. 9) and shows the basic fault structure, but as we compare the color bar scale with other horizons, it shows the amplitude difference between H3

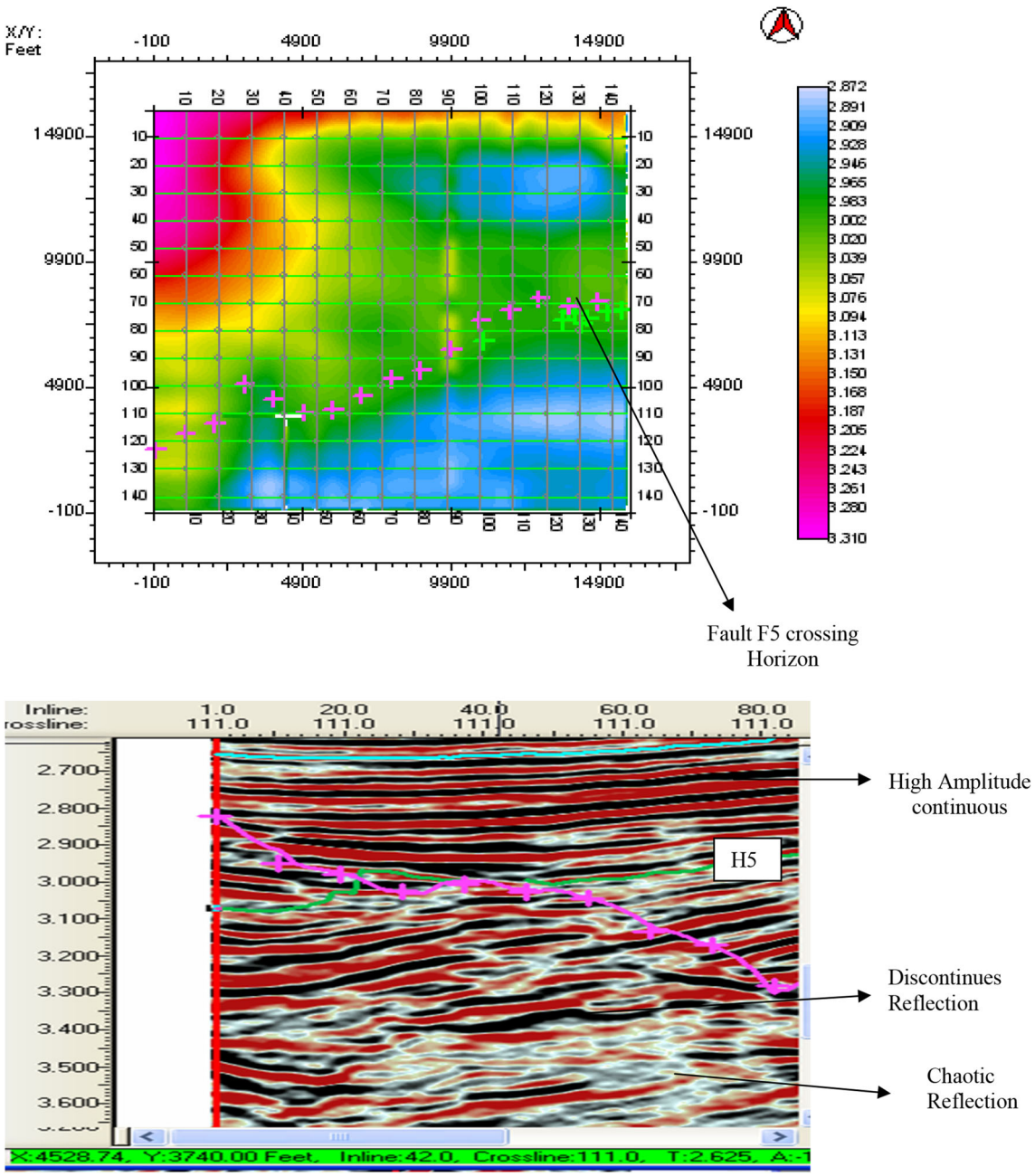

Fig. 8 Travel time of horizon H5 at 23.55 s., with master faults continue, continuous to discontinuous reflection with high and low amplitudes and chaotic area

and H2. By this, we interpreted the uplifts and some low-to-high-amplitude thickness areas.

Amplitude window H3 ±0.05

Basically, this map shows the amplitude at above 0.05 s and below 0.05 s to get any window or anticline feature as shown in Fig. 10.

Time-thickness map

This map shows the basic structure and the thickness as compared to the time of reflection of seismic waves as in Fig. 11. The map has the following characteristics.

- Needs two bounding surfaces.
- Shows the interval thickness.

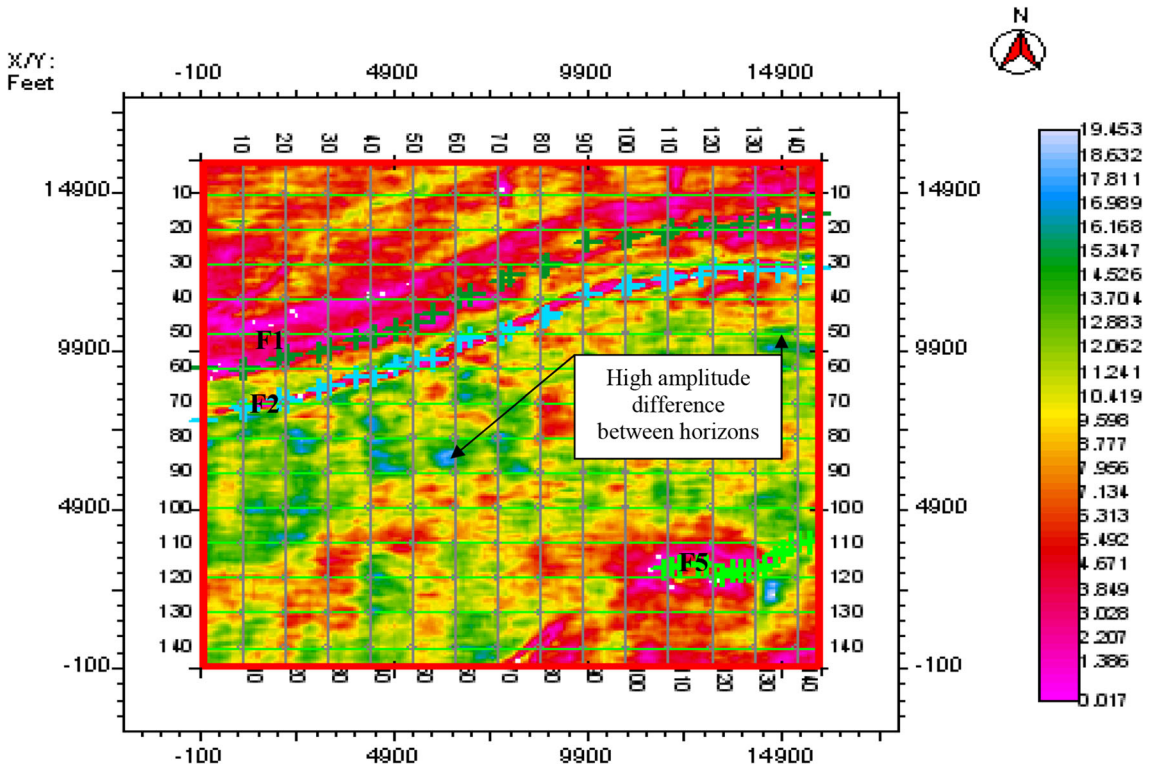

Fig. 9 The amplitude map in between horizon H3 and H2, whereas the *color bar* shows the fluctuation in amplitude in between these horizons

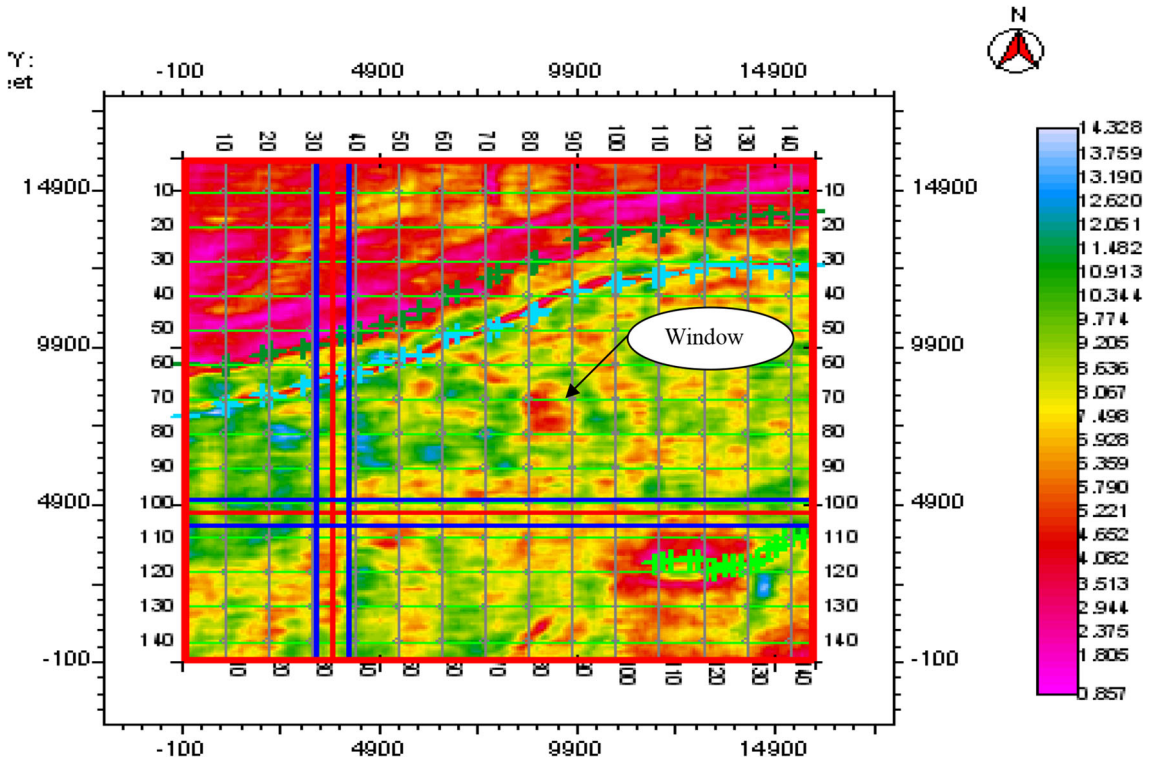

Fig. 10 The horizon H3 with ±0.05 s., amplitude to show the window

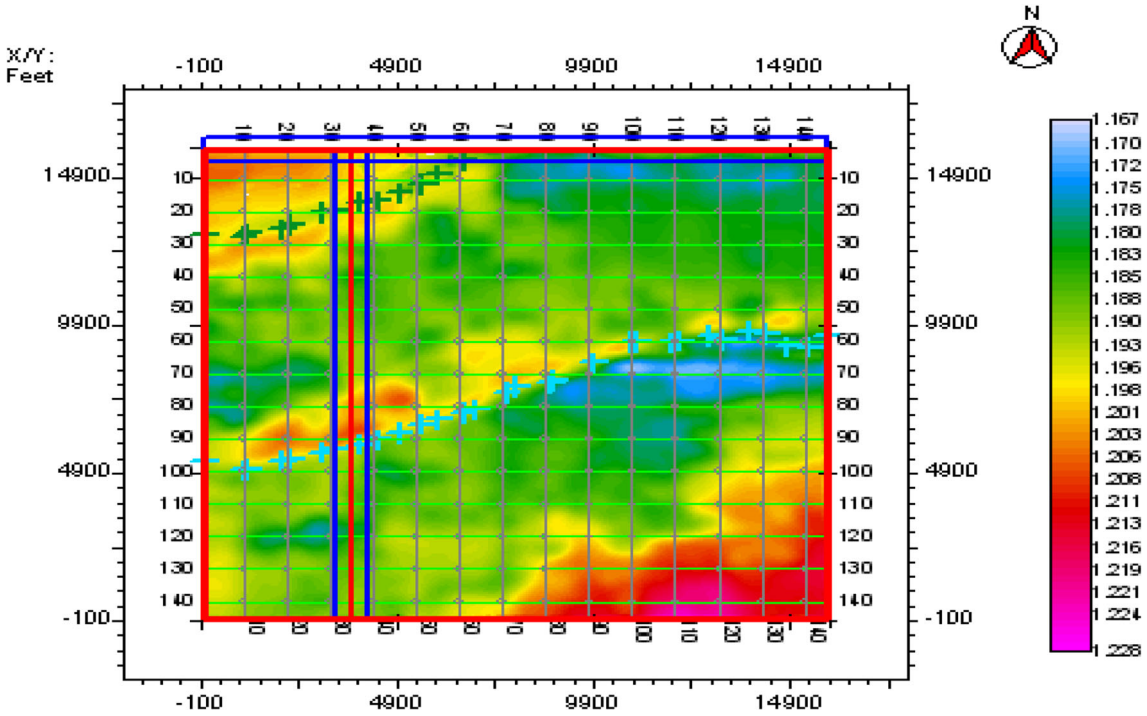

Fig. 11 The time thickness between horizon H3 and H1, but as there is now such thickness changes in between the horizons so the color bar does not much variation in time

Fig. 12 Contour map over time structure map of horizon H3, map distribute with line that shows the different travel time of reflection area

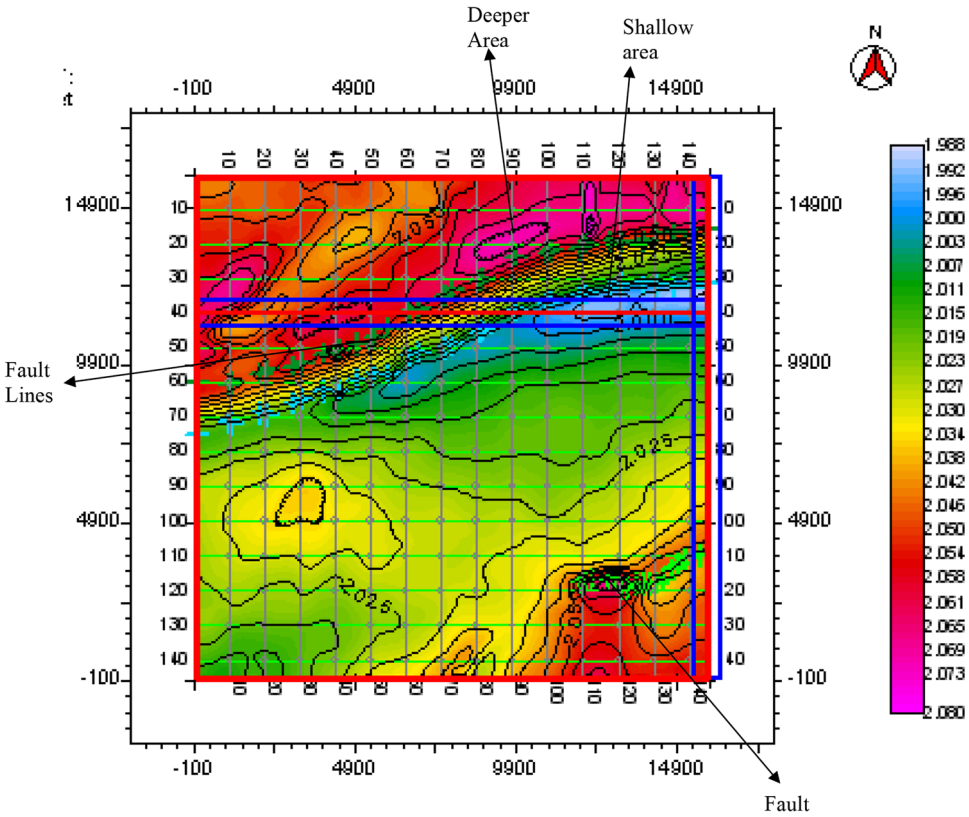

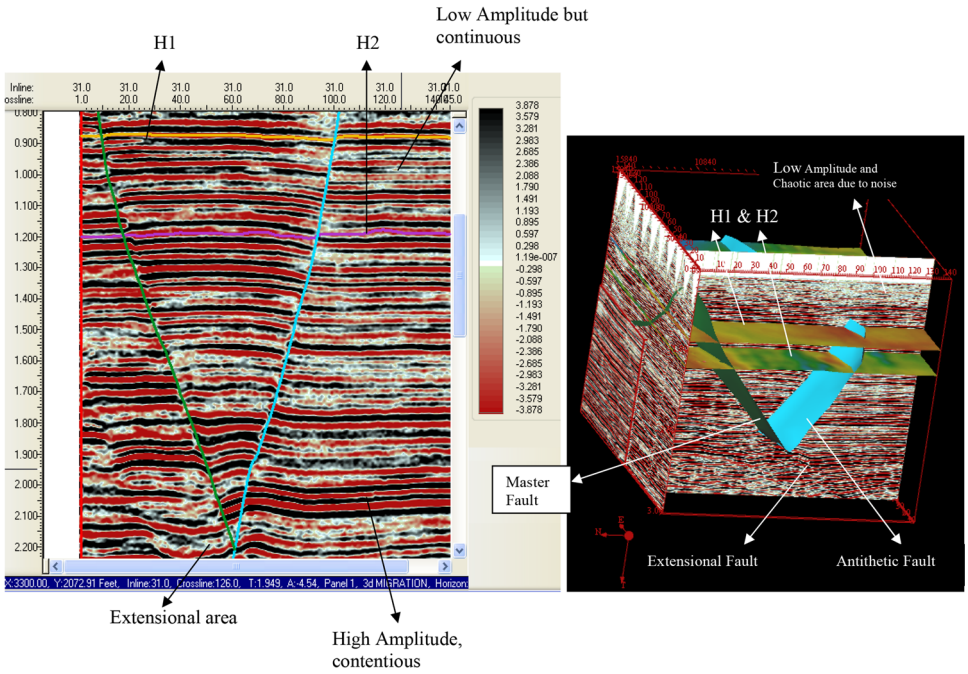

Fig. 13 Fault F1 (master) and fault F2 (antithetic) cut across the horizon H1 and H2, and some extensional area crosses by fault

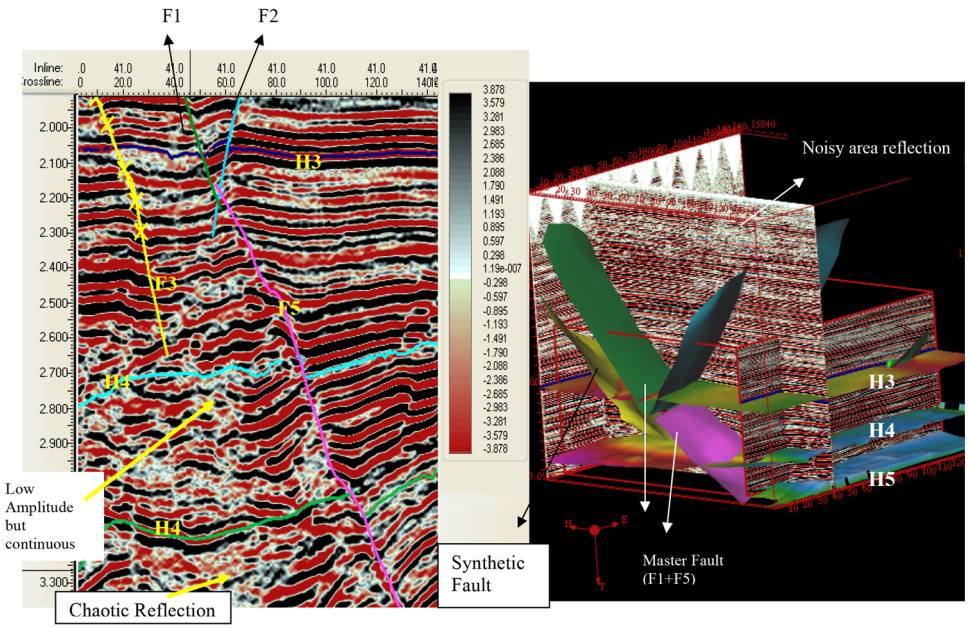

Fig. 14 Fault F3 (synthetic), faults F4 and F5 where fault F4 is continuous of fault F1 cut across the horizon H3, H4 and H5, and some extensional area crosses by fault with chaotic reflection

- Reservoir total thickness, sedimentary units, whole formation thicknesses.
- Can be draped on time structure maps.
- Calculating volumetric.
- Can be combined with amplitude maps to show where they are thick, high-amplitude sediment bodies.

Time-thickness map between H2 and H1

See Fig. 11.

Contour map

The contour shows the elevated and deep area that is related to the time structure map. It also shows the fault lines that crosses the seismic lines. Here the contour shows the shallower part with blue and the deeper part with pink as seen in the color bar scale in Fig. 12.

Faults crossing horizons

In our interpretation, we selected five faults. Fault F1 and fault F2 (normal fault) cut across the first two horizons, H1

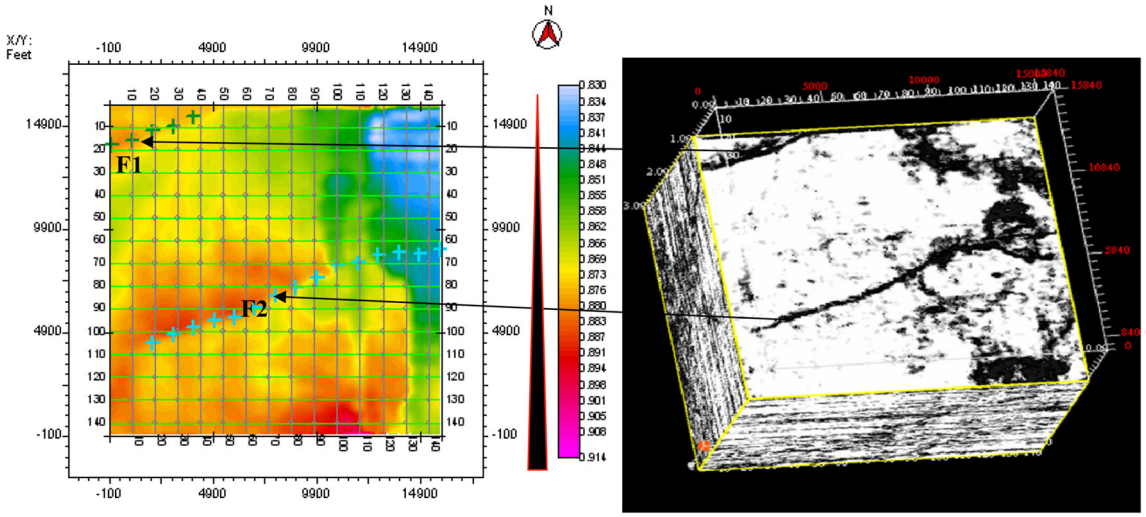

Fig. 15 The comparison of horizon H1 with coherence map to show clear picture of faults F1 and F2

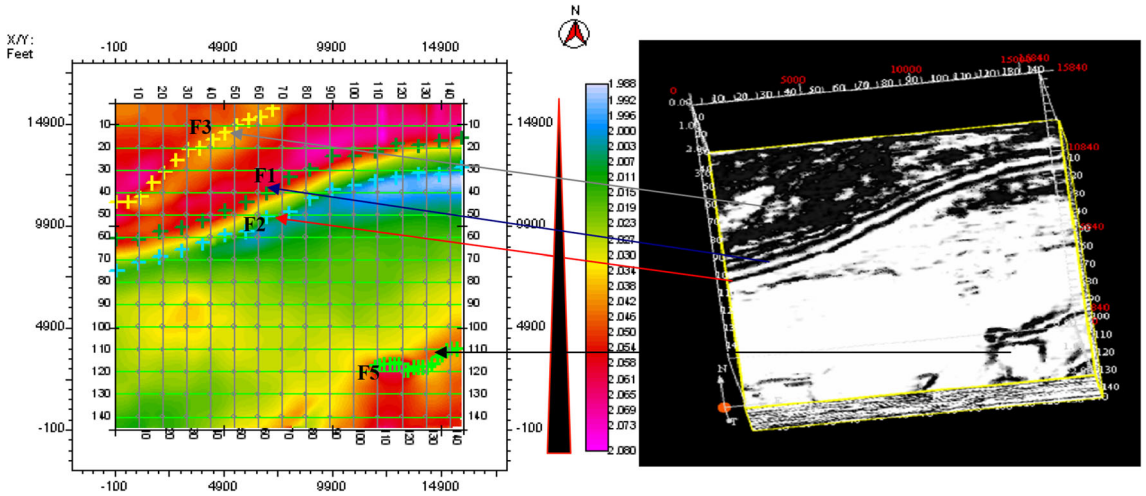

Fig. 16 The comparison of horizon H3 with coherence map to show clear picture of faults F1, F2, F3 and F5

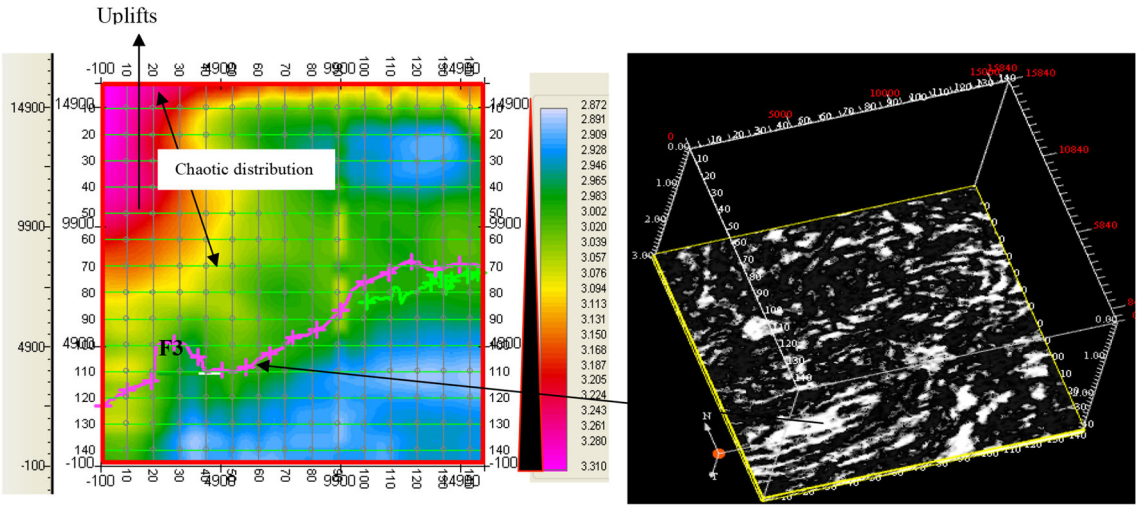

Fig. 17 The comparison of horizon H3 with coherence map to show amplitude difference due to uplifts at bottom

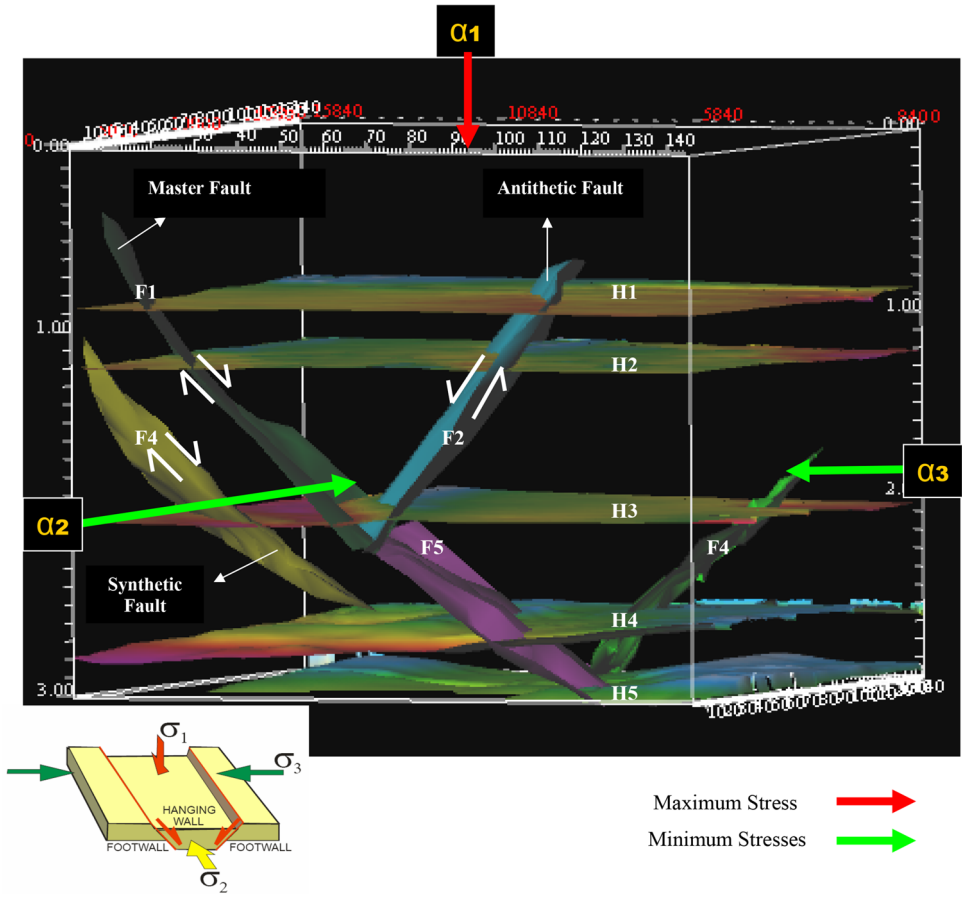

Fig. 18 Simple fault model with minimum and maximum stresses with the compression of horizons selected

and H2, with little variation in time-thickness variation as in Fig. 12, whereas fault F3, fault F4 and fault F5 (which is continuity of fault F1 as an extensional fault at bottom) cut across the last three horizons. So fault 1 + 5 is the *major fault*, fault F2 is the *antithetic fault,* and fault F3 is the *synthetic fault*. There is also other number of faults that cut across each other in the form of conjunction of faults (Figs. 13, 14, 15).

Coherence map

Coherence map here shows the contrast of faults that cut across the horizon. It does not show the amplitude and time of reflection. Figures 9 and 10 show the fault in coherence map crossing horizon H1 and H2. It shows the black and white contrast of chaotic area and the fluctuation in amplitudes (not its value) in some areas like in Fig. 11. The characteristics of this map are:

- Used to show faults, channels, landslides, salt structures.
- Not able to show amplitude contrasts.
- Derived from breaks or discontinuities in the seismic peaks or troughs.

Geological fault model

A simple geological model was generated from this project as shown in Fig. 16. The model shows the five horizons and the fault morphology over horizons. It also shows the major fault (normal fault) cut across the whole cube in inline as well as in crossline called the master fault. The antithetic fault dipping down at about 60° also cut across the seismic line and is ~2.3 s deep. There are also some uplifts and extensional system of fault at the bottom of the cube that may be related to gas accumulation in between the fault, wavy region and rotational area. The entire interpreted fault indicates normal displacement, but there is also some rotational area at the bottom of the major fault (Fig. 17).

The main stresses that cause the cube faulted in conjunction of fault are shown in Fig. 18 that shows the maximum and minimum stress in particular directions.

Conclusion

Based on the entire selected horizons, constructed maps and dominant fault construction model, the main conclusions drawn are;

- Postkinematics deposition at top shows low amplitude and moderate chaotic area due to different sediment depositions, or it may be due to noise at the surface during seismic wave generation.
- Fault sets are master, antithetic and synthetic.
- Irrigational faults i–e normal, conform by the discontinuity of seismic line at the top, whereas some rotation occurs at the bottom of the same major fault.
- Ductile deformations at the bottom due to some lose sediment show the fluctuation of amplitude in seismic lines.
- Pair of faults with opposite sense of shear (dip direction and angle at 60°), which crosscut each other and the horizons.
- Once fault is occur, the surrounding rock become weak enough to generate major fault in future is or deformation occur for long period.
- Footwall of major fault during extension clear at the bottom with some distorted i–e chaotic are shows (maybe) due to gas trap reflection.
- The maximum stress occurs at the top.

Generally, continuity of the horizons (top three horizon) is good and at the bottom (last two horizon) is poorly traced due to possible occurrence of gas in some area which makes the reflectors fuzzy and amplitude very poor. The geological complexity also results in poor images within the fault zone; consequently, interpretation is difficult to establish. At the top-most seismic area, the reflection is also very poor and that may be due to noise during seismic wave generation. Therefore, the use of 3D visualization with horizon attributes can provide easily understood displays of massive amounts of data. These displays can provide insight into relationships between attributes of horizons and can reveal faulting and structural details far more effectively than 2D maps as compared to 3D visualization.

Acknowledgements The authors would like to thank the Norway Ministry of Petroleum and Energy for providing 3D seismic data of Gullfaks field, block 34/10 in the Norwegian sector of the North Sea.

References

Anderson EM (1951) The dynamics of faulting. Oliver & Boyd, Edinburgh

Anthony MS, Per IB, Lone Dyrmose C, Rune F, Marie K, Kvadsheim E, Knight I, Rye-Larsen M, Williams J (2008) Petroleum geoscience in Norden—exploration, production and organization. Episodes 31(1):115–124

Arild H, Petter E (2000) Introduction to the Gullfaks area. Statoil

Bacon M, Simm R, Redshaw T (2007) 3-D seismic interpretation. ISBN: 9780521710664

Bækken J, Zenker E (eds) (2007) The Norwegian petroleum sector. Ministry of Petroleum and Energy, Oslo

Beach A (1986) A deep seismic reflection profile across the northern North Sea. Nature 323:53–55

Erichsen T, Helle M, Henden J, Rognebakke A (1987) In: Spencer AM, Campbell CJ, Hauslien SH, Nelson PH, Nysæther E, Ormaasen EG (eds) Gullfaks, geology of the Norwegian oil and gas fields. Graham & Trotman, London, pp 283–286

Evans D, Graham C, Armour A, Bathurst P (eds) (2003) The Millennium Atlas: petroleum geology of the central and northern North Sea. The Geological Society, London

Fossen H (1989) Indication of transpressional tectonics in the Gullfaks oil-field, northern North Sea. Mar Pet Geol 6:22–30

Fossen H, Hesthammer J (1998) Structural geology of the Gullfaks field, Northern North Sea. In: Coward, M. P., Daltaban, T. S., Johnson, H. (eds) Structural geology in reservoir characterization. Geological Society, London, Special Publications, 127, 231–261

Fossen H, Hesthammer J (2000) Possible absence of small faults in the Gullfaks Field, northern North Sea: implications for downscaling of faults in some porous sandstones. J Struct Geol 22:851–863

Fossen H, Rornes A (1995) Properties of fault populations in the Gullfaks field, northern North Sea. J Struct Geol 18:179–180

Gabrielsen RH, Faerseth RB, Steel RJ, Idle S, Klovjan OS (1990) Architectural styles of basin fill in the northern Viking Graben. In: Blundell DJ, Gibbs AD (eds) Tectonic evolution of the North Sea Rifts. Clarendon, Oxford, pp 158–183

Koestler AG, Buller AT, Milnes AG, Olsen TS (1994) A structural simulation tool for faulted sandstone reservoirs: exploratory study using field data from Utah and Gullfaks. In: Aasen JO et al (eds) North Sea oil and gas reservoirs—IIL. Kluwer, Dordrecht, pp 157–165

Milnes AG, Storli A (1992) Complex hanging-wall deformation above an extensional detachment—example: Gullfaks Field, northern North Sea. In: Larsen RM et al (eds) Tectonic modelling and its application to petroleum geology. NPF Special Publication 1. Elsevier, Amsterdam, pp 243–251

Norwegian Petroleum Directorate (2007) The petroleum resources of the Norwegian continental shelf. Norwegian Petroleum Directorate, Stavanger

Perkins H (1961) Fault closure-type fields, Southeast Louisiana. Gulf Coast Assoc Geol Soc Trans 1:177–196

Petterson O, Storli A, Ljosland E, Massie I (1990) The Gullfaks field: geology and reservoir development. North Sea oil and gas reservoirs—II Norwegian Institute of Technology. Graham and Trotman, London, pp 67–90

Petterson O, Storli A, Ljosland E, Nygaard O, Massie I, Carlsen H (1992) The Gullfaks field: Chapter 27. In: M54: giant oil and gas fields of the decade 1978–1988. AAPG Search and Discovery, Special Publication, pp 429–446

Rouby D, Fossen H, Cobbold P (1996) Extension, displacements and block rotations in the larger Gullfaks area, northern North Sea, as determined from plan view restoration. AAPG Bull 80:875–890

Sebring L Jr (1958) Chief tool of the petroleum exploration geologist: the subsurface structural map. AAPG Bull 42:561–587

Smalley PC, Stephen HB, Michael N, Johnsen S, Antonella G (2008) Handling risk and uncertainty in petroleum exploration and asset management: an overview. AAPG Bull 92(10):1251–1261

Statoil Hydro (2007) Reservoir management plan for Gullfaks. GF RESU-HF-07 0122

Wensaas L, Shaw HF, Gibbons K, Aagaard P, Dypvik H (1994) Nature and causes of overpressuring in mudrocks of the Gullfaks Area, North Sea. Clay Miner 29:439–449

Yielding G, Overland JA, Byberg G (1999) Characterization of fault zones for reservoir modelling: an example from the Gullfaks Field, northern North Sea. Bull AAPG 83:925–951

Zanella E, Coward MP (2003) Structural framework. In: Evans D, Graham C, Armour A, Bathurst P (eds) The Millennium Atlas: petroleum geology of the central and northern North Sea. The Geological Society, London, pp 45–59